Formation of carbon capsules from an amorphous carbon film by Ga and Ni/Co catalysts in a transmission electron microscope

Cheng-Yu Wang, Yen-Chih Chen, and Wen-Huei Chu
Department of Materials Science and Engineering, National Cheng Kung University, Tainan, Taiwan 701

Chuan-Pu Liu[a)]
Department of Materials Science and Engineering, National Cheng Kung University, Tainan, Taiwan 701; and Center for Micro/Nano Science and Technology, National Cheng Kung University, Tainan, Taiwan 701

C.B. Boothroyd
Institute of Materials Research and Engineering, 3 Research Link, Singapore, 117602

(Received 28 June 2008; accepted 24 November 2008)

Direct conversion of an amorphous carbon (C) film to capsules by gallium (Ga), and nickel and cobalt (NiCo) alloy particles upon heating is investigated in situ by transmission electron microscopy (TEM). Capsules are catalyzed in an NH_3 atmosphere when the temperature is raised to 1050 °C. High resolution TEM reveals that graphene flakes initially nucleate at the surface of the catalysts, then segregate and transform into faceted multi-shell capsules upon continued heating. The solubility of carbon in the NiCo alloy particles can be differentiated from the solubility of carbon in Ga particles by the thickness of the walls. The C/Ga binary phase in nanoparticles is discussed regarding the formation of thin-walled carbon capsules.

I. INTRODUCTION

Carbon nanocapsules are zero dimensional structures consisting of carbon shells wrapping solid cores. When the shells wrap transition metal crystals of nanometer size, the core-shell structures offer promising potential in high-density data storage[1] and in vitro applications.[2] One of the advantages of carbon shells is that they protect core crystals, typically iron-group metals, from oxidizing and etching. Carbon capsules have been synthesized by chemical vapor deposition (CVD),[2] arc discharge,[3,4] and radio frequency plasma torch.[5]

The carbon products synthesized by arc discharge include not only nanocapsules, but also nanotubes,[6,7] nanoparticles,[8,9] and nanocages.[10] Many metals have been used as catalysts when using arc discharge and laser vaporization to grow core-shell structures, including transition metals of Sc,[11] Y,[12] Fe,[13] and the lanthanide metal La.[14] Seraphin et al.[15] systematically categorized elements into the four groups commonly used for manufacturing core-shell nanostructures by arc discharge. In the first group, the core is in the form of carbides and consists of B, V, Mn, Y, Zr, Nb, Mo, and La. In the second group, the core, which cannot be encapsulated but tolerates the formation of carbon cages, consists of Cu, Zn, Pd, Ag, and Pt. In the third group, the core has a strong potential that forms stable carbides and competes with the formation of cages, and consists of Al, Si, Ti, Sn, and W. The last group consists of the iron group transition metals, Fe, Co, and Ni, which can stimulate the formation of filled and/or unfilled tubules, beads, and cages. In addition to arc discharge, carbon nanocapsules have been synthesized by using copper phthalocyanine (CuPc) as the precursor in the CVD.[16] Pseudohexagonal carbon or silicate nanocases with a different morphology have also been synthesized by mesoporous templates, and interesting applications to component separation and drug delivery have been demonstrated.[17–20] The synthesis of ultrasmall carbon capsules and thin-walled shells are still being pursued.[21]

Carbon nanostructures have been commonly analyzed by transmission electron microscopy (TEM) to reveal morphology, microstructure, elemental identification, and mapping. Simultaneously, TEM has also been used to study carbon structures dynamically, including the formation of capsules from Al- and Au-C core-shell structures in vacuum[22,23] and capsules from Ni-C in a hydrogen atmosphere,[24] and hollowing Ni-caged capsules[25] and converting carbon onions to diamond crystals.[26]

The complexity and extreme conditions involved in arc discharge and CVD make the nucleation and growth mechanisms of carbon capsules difficult to understand fully. Here, by extending the materials of interest and

[a)]Address all correspondence to this author.
e-mail: cpliu@mail.ncku.edu.tw
DOI: 10.1557/JMR.2009.0166

focusing on the in situ inspection of the evolution of products grown by gallium (Ga) particles and nickel and cobalt (NiCo) alloy particles in an NH_3 atmosphere on an amorphous carbon-coated grid in a TEM, we have found that thin-shelled nanocapsules can be catalyzed by Ga.

II. EXPERIMENTAL METHOD

The in situ growth and analyses were carried out on an ultrahigh vacuum JEM2000V (Japan) TEM (1×10^{-9} Torr), which was operated at 200 keV. This microscope is fitted with an LaB_6 gun, electron beam evaporators, a gas inlet, a charge couple device (CCD) camera and a Gatan Imaging Filter (GIF; Pleasanton, CA). The catalysts used in the experiment included Ga, Ni, and Co. Ga droplets were first placed on an amorphous carbon-coated Mo grid which was then glued onto an Si substrate through which a current was passed to heat the specimen grid. The Si substrate was thinned until perforation using a dimpler. After loading the substrate in the TEM, Ni and Co were codeposited from separate electron beam evaporators at room temperature. Subsequently, the grid was gradually heated from room temperature to 1050 °C. When the temperature reached 850 °C, NH_3 was injected with the pressure held at 6×10^{-6} Torr. During this process, an area containing Ga droplets was observed on a TV rate camera and recorded on videotape.

For comparison, we also performed two additional in situ growth experiments using only Ga particles or Ga and Ni alloy particles as catalysts separately on a JEOL JEM2010 TEM fitted with a LaB_6 gun, operated at 200 keV and a CCD camera at a TV scanning rate. In the former case, the Ga particles were placed on a carbon-coated Mo grid. In the latter case, the Ni particles were deposited on a carbon-coated Mo grid by an electron beam evaporator, and the Ga particles were then placed on the same grid. The heating process was done with a Gatan heating holder up to 900 °C. TEM post analysis was performed with the same microscopes as well as with a JEOL JEM2100F, operated at 200 keV, fitted with CCD cameras and a GIF.

III. RESULTS

Selected snapshots representative of the evolution of Ga particles, alloy particles and the formation of carbon capsules during heating are shown in Fig. 1. Figures 1(a) and 1(b) show a large Ga particle disintegrating into smaller particles and the distribution of NiCo alloy particles at 850 °C and 1000 °C, respectively. Figure 1(c) shows hollow and catalyst-caged capsules at 1050 °C. During heating, the Ga particles remained liquid with high fluidity, which caused the image contrast to change continuously. The size of the Ga particles also decreased due to evaporation as the temperature was increased. In contrast, the size of the alloy particles increased slightly, while their area density reduced from 10×10^{11} cm^{-2} down to 5×10^{11} cm^{-2} when the temperature was raised from 850 °C to 1000 °C. The yield of the carbon capsules may be relatively lower than the commonly used methods probably due to limited carbon source.

Possible catalysts for the capsule formation in this study included NiCo alloy particles, alloy-Ga core-shell particles, and Ga particles, as shown in Fig. 1(b). Different morphologies of capsules are shown in Fig. 1(c), including filled, partially-filled, and hollow capsules, as indicated by the arrows in the figure. More variants are shown in Fig. 2. Figures 1(c) and 2 reveal that the graphene shells take the shape of the catalysts. Because of the different size distribution of the different catalysts, medium-sized capsules were catalyzed from NiCo alloy or alloy-Ga core-shell particles, as shown in Figs. 2(a) and 2(b), while larger-sized capsules were formed from Ga particles, as shown in Figs. 2(c) and 2(d). The wall thickness of the capsules varied from 2 to 12 nm, as shown in Fig. 2(e), and the distribution of the core diameter of the capsules had two maxima at 20 nm and 30 nm, as shown in Fig. 2(f), corresponding to the capsules catalyzed from NiCo alloy particles and Ga or compound particles, respectively. The ratio of the wall thickness to the capsule diameter from statistical analysis shows three peaks, which are at 0.12, 0.17 to 0.26, and >0.3. The first group is characterized by ultra-thin

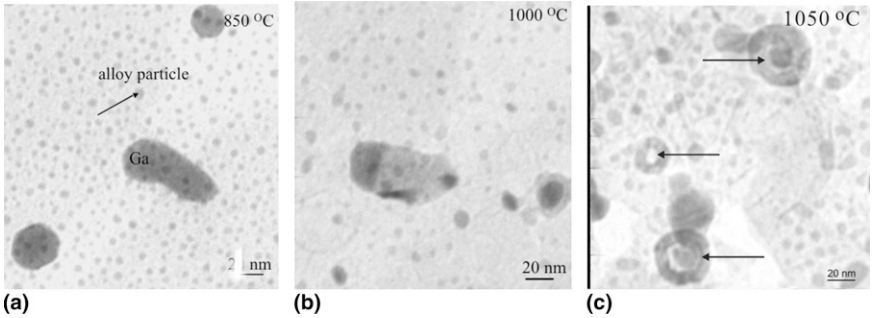

FIG. 1. Snapshots reproduced from a video of TEM images showing Ga particles, NiCo alloy particles, and carbon capsules at (a) 850 °C, (b) 1000 °C, and (c) 1050 °C during heating.

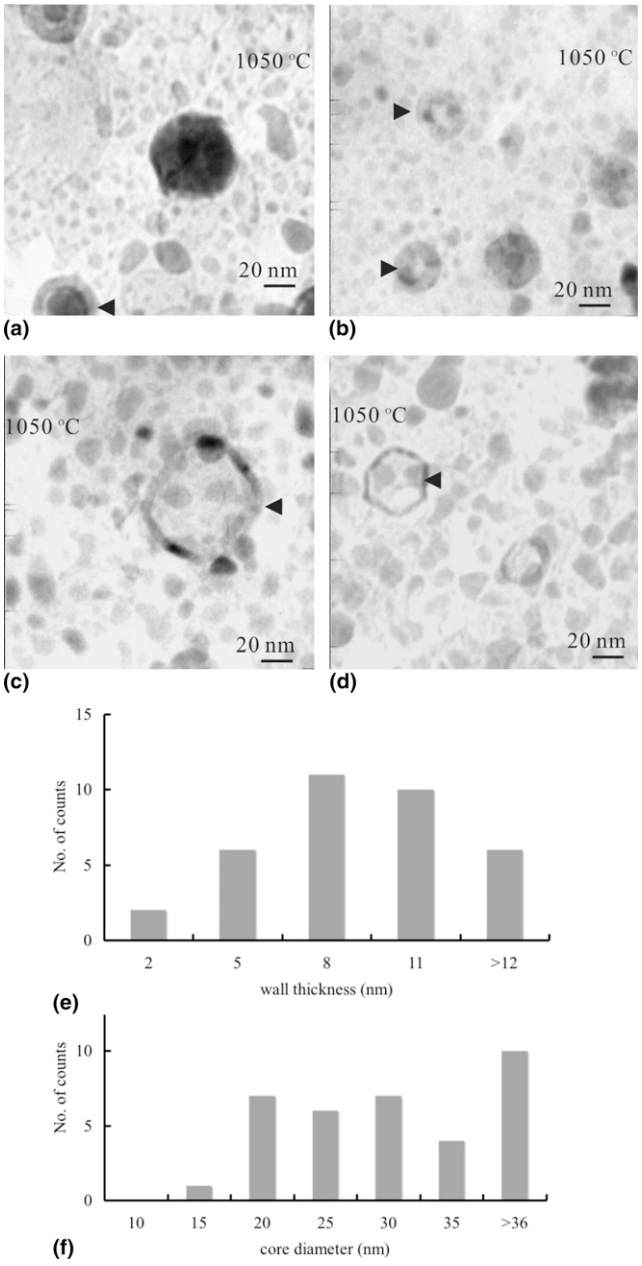

FIG. 2. TEM images showing the variety of morphologies of synthesized carbon capsules. (a) A quasi-spheroidal capsule around a trapped catalyst, indicated by the arrowhead, (b) hollow capsules, and (c, d) polyhedral capsules. (e) Statistical analysis of wall thickness and (f) core diameter of the capsules.

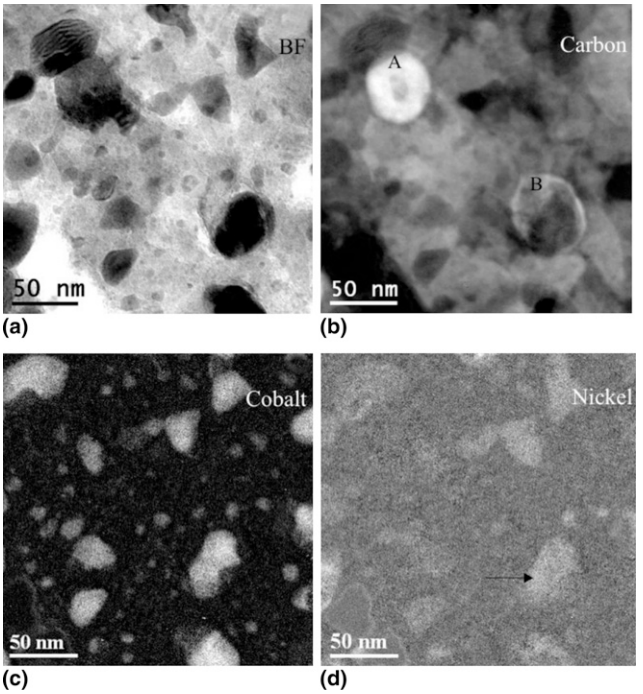

FIG. 3. TEM images of typical capsules. (a) A bright-field image and elemental maps of (b) carbon, (c) cobalt, and (d) nickel.

walls formed around large catalyst particles, consistent with the particle being Ga particles, while the latter two groups should be related to the NiCo alloy particles.

To determine the state of alloy particles at 1050 °C, images were carefully checked for diffraction contrast, but such an approach was insufficient and made it difficult to demonstrate that the smaller alloy particles were crystalline. Hence, the melting temperature (T_m) of the alloy particles was estimated theoretically following the analyses of Jiang et al.[27] According to the phase diagram,[28] the melting temperatures (T_m) of bulk Ni, Co, and NiCo alloy are 1455 °C, 1500 °C, and nearly 1500 °C, respectively. Due to the size effect, T_m would be reduced, and the critical particle size of NiCo alloy for melting at 1050 °C is about 6 nm. Therefore, it is supposed that the alloy particles are solid.

The distribution of elements in the particles was investigated using energy-filtered imaging. A bright field (BF) image and C, Co, and Ni elemental maps are shown in Fig. 3. The carbon map clearly exhibits two capsules, indicated by the letters A and B, and shows that the wall thickness of capsule A is much larger than that of capsule B. By comparing the BF image [Fig. 3(a)] with the C and Ni maps [Figs. 3(b) and 3(d)], it can be seen that there is a tiny alloy particle remaining at the core of capsule A with another alloy particle overlaying the wall of this capsule, while capsule B partially encapsulates another alloy particle. It is likely that capsule B formed around an alloy-Ga core-shell catalyst particle from which the Ga particles evaporated, leaving a hole and an alloy particle behind.

High resolution TEM images of the capsules are shown in Fig. 4, where Figs. 4(a), 4(b), and 4(c) show an as-grown capsule, a partially-filled capsule, and a faceted cage, respectively. For the as-grown capsule [Fig. 4(a)], disordered graphene flakes have grown around the particle, while for the partially-filled and hollow capsules, they are crystalline, and the graphene lattice spacing of the capsule in Fig. 4(c) is 0.34 nm over

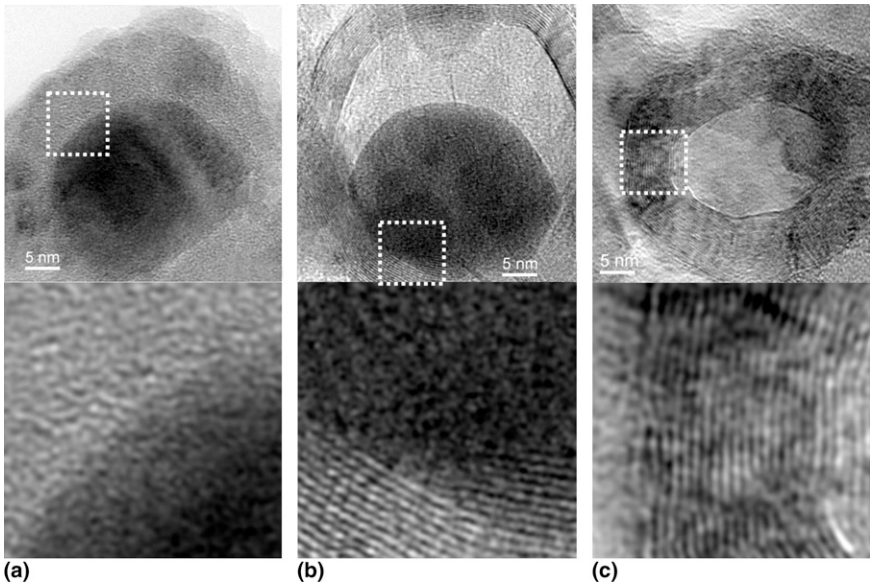

FIG. 4. HRTEM images and the enlarged images from the respective marked regions of (a) a catalyst-trapped capsule, (b) a partially-filled capsule, and (c) a hollow-core capsule.

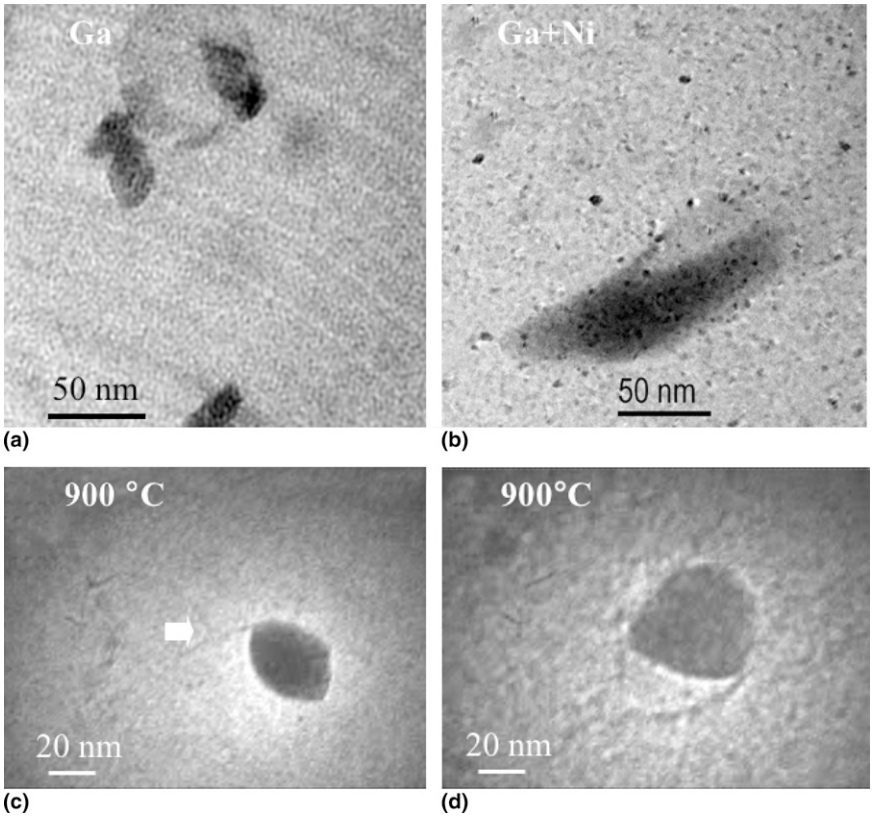

FIG. 5. BF images (a) Ga particles and (b) Ga-Ni particles on the amorphous carbon film at room temperature. Snapshot reproduced for (c) heating Ga particle at 900 °C and for (d) heating Ga-Ni particles at 900 °C.

the entire thickness range. Figure 4(b) shows that the graphene layers have grown epitaxially on the catalyst, which has a spacing of 0.35 nm, subject to (100) of primitive cubic CoC_x carbide.[29]

To confirm the role of Ga in the carbon capsule formation, two more in situ experiments were performed and the results are shown in Fig. 5, with the left and right panels acquired from the TEM grid with Ga

particles alone, and Ga/Ni particles, respectively. Figures 5(a) and 5(b) show the BF image of the as-deposited Ga particles and the Ga/Ni particles on an amorphous carbon film, respectively. Figures 5(c) and 5(d) show snapshots of the two samples when the temperature was raised to 900 °C. The catalytic power of pure Ga particles is obviously reduced, and only ultrathin graphene flakes are formed, as indicated in Fig. 5(c). On the other hand, the Ga/Ni particles are capable of catalyzing carbon capsules and, during growth, Ga escapes out of the capsules due to evaporation, leaving behind a hollow core in the capsule, as shown in Fig. 5(d).

IV. DISCUSSION

Compared with the equilibrium vapor pressure of close to 7×10^{-4} Torr at 1000 °C for Ga, the TEM chamber was kept at 1×10^{-9} Torr. However, Ga particles remained up to 1000 °C, as shown in Fig. 1(b), indicating that graphene flakes catalyzed at the surfaces of Ga particles could slow down evaporation. Ga atoms could evaporate and escape from a capsule at temperatures higher than 950 °C. Due to their larger initial size, the Ga particles synthesized large cages, as shown in Figs. 2(c) and 2(d).

In JEM2000V and JEM2010, the emission current at 200 keV was set to 109 μA and the microscope condenser aperture limited the irradiated area. The electron dose was calculated to be less than 100 A/cm^2, which was less than the 150 A/cm^2 required to form spherical onions.[30] Hence, the effects from electron beam irradiation were relatively minor.

In the literature, carbon nanostructures have been catalyzed through the vapor-solid-solid (VSS) mechanism, in situ observed by Hoffman et al.,[31] from which carbon atoms dissolve in solid precursors, undergo bulk and/or surface diffusion, and then segregate from the supersaturated precursors to form carbon nanostructures. In contrast, in the immiscible system, including Al-C[22] and Au-C,[23] crystalline Al and Au nanoparticles also catalyze carbon capsules. Although there is no phase diagram available for Ga-C,[28] in our study, Ga particles and NiCo-Ga core-shell particles catalyzing carbon capsules were in situ observed and demonstrated. The carbon source is supplied by redeposition from the TEM chamber and/or diffusion from the amorphous carbon film. Hence, we speculate that carbon atoms exhibit relatively low solubility and/or immiscibility in Ga, and physorbed carbon atoms on the surface of Ga particles are catalyzed to form graphene flakes. Therefore, two catalyst-dependent nucleation and growth mechanisms are proposed for the formation of multi-shell capsules in this study, as shown in Fig. 6. In addition, NiCo alloy particles can be either liquid or solid, depending on their sizes, which causes variations in the morphology of the nucleated graphene layers. For liquid NiCo alloy particles, oversaturated carbon forms disordered graphene flakes and nucleates at the surface of the catalyst particles, as shown in Fig. 6(a), and takes the shape of particles. Subsequently, the disordered flakes convert to epitaxial faceted shells upon annealing, as shown in Fig. 6(b), and additional carbon is supplied and segregated from the catalyst particles to form the multi-shell capsules, as shown in Fig. 6(c). Upon continued heating, catalyst atoms gradually diffuse out of the capsules through defects in the shells and the pathways between the shells, resulting in hollow and catalyst-trapped capsules. For solid NiCo alloy particles, the process follows the steps proposed for the liquid phase, except that ordered graphene flakes initially nucleate on the surface of the alloy crystals, resulting in the growth

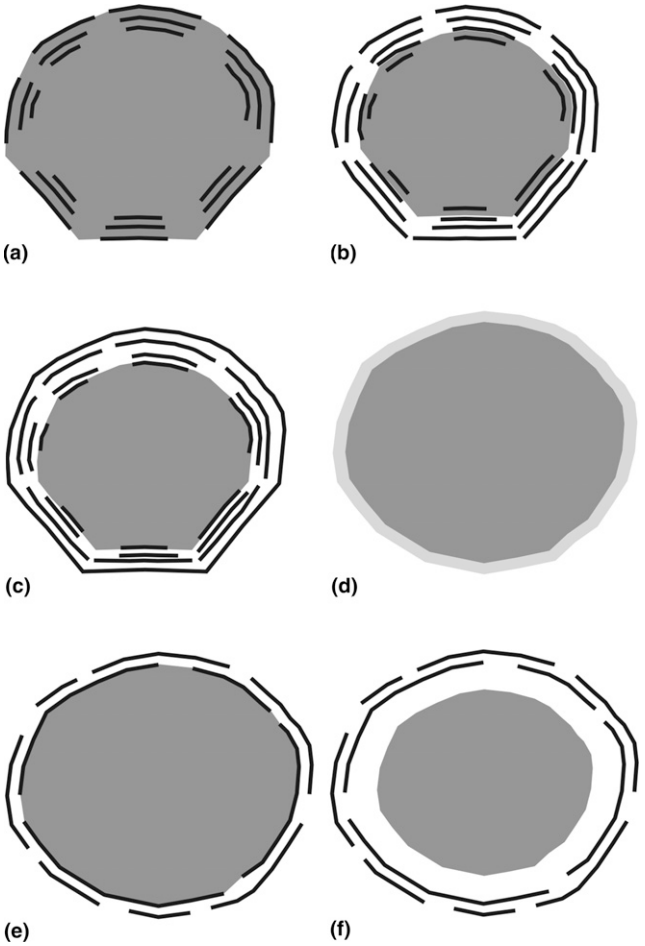

FIG. 6. Schematic illustration of nucleation and growth mechanisms of alloy particles and Ga particles catalyzing carbon capsules. (a) Graphene flakes nucleate at the surface of an alloy particle, (b) the flakes connect and wrap around the alloy particles, (c) graphene shells segregate from the alloy particle, changing into a partially-filled capsule. (d) Carbon atoms are physorbed on the surface of a Ga particle, (e) the physorbed carbon layer is catalyzed to form graphene flakes, and (f) a partially-filled capsule is observed due to Ga evaporation out of the core.

of epitaxial faceted layers directly. For Ga particles, carbon atoms are absorbed on the Ga surface, as shown in Fig. 6(d), and are converted into disordered flakes, as shown in Fig. 6(e). Such flakes also convert to faceted multi-shell capsules upon annealing, but the thickness is much smaller since the growth would terminate without an additional carbon supply. As the process continues, the Ga particles shrink due to evaporation, as shown in Fig. 6(f), and eventually hollow capsules result. Consequently, capsules synthesized from either alloy or Ga particles will eventually be converted to faceted shells upon annealing, while their thickness is determined by the solubility of carbon in the catalyst particles.

V. CONCLUSION

We have demonstrated that Ga and NiCo particles catalyze carbon capsules from an amorphous carbon thin film on heating in a TEM. Both phases grow carbon capsules via different growth mechanisms but the catalytic power of NiCo is superior to that of Ga particles. The NiCo-Ga core-shell nanoparticles change the solubility of C in this structure and, in turn, improve the catalytic power to synthesize thicker wall capsules than those from Ga particles alone.

ACKNOWLEDGMENTS

The authors are grateful to IMRE (Singapore) for the use of the JEOL-2000V in situ TEM and the Center for Micro/Nano Technology Research, National Cheng Kung University, Taiwan, for access to equipment and the provision of a student scholarship for C.Y. Wang. In addition, we would also like to thank Dr. Dunin-Borkowski for interesting and reflective discussions and Drs. Y.L. Foo and M. Lin for their assistance in the operation of the JEOL-2000V.

REFERENCES

1. C. Desvaux, C. Amiens, P. Fejes, P. Renaud, M. Respaud, P. Lecante, E. Snoeck, and B. Chaudret: Multimillimetre-large super lattice of air-stable nanoparticles. *Nat. Mater.* **4,** 750 (2005).
2. W.S. Seo, J.H. Lee, X. Sun, Y. Suzuki, D. Mann, Z. Liu, M. Terashima, P.C. Yang, M.V. McConnell, D.G. Nishimura, and H.J. Dai: FeCo/graphitic-shell nanocrystals as advanced magnetic-resonance-imaging and near-infrared agents. *Nat. Mater.* **5,** 971 (2006).
3. J. Jiao, S. Seraphin, X. Wang, and J.C. Withers: Preparation and properties of ferromagnetic carbon-coated Fe, Co, and Ni nanoparticles. *J. Appl. Phys.* **80,** 103 (1996).
4. J.J. Host, J.A. Block, K. Parvin, V.P. Dravid, J.L. Alpers, T. Sezen, and R. LaDuca: Effect of annealing on the structure and magnetic properties of graphite encapsulated nickel and cobalt nanocrystals. *J. Appl. Phys.* **83,** 793 (1998).
5. Z. Turgut, J.H. Scott, M.Q. Huang, S.A. Majetich, and M.E. McHenry: Magnetic soft magnetic materials. *J. Appl. Phys.* **83,** 6468 (1998).
6. S. Iijima: Helical microtubules of graphitic carbon. *Nature* **354,** 56 (1991).
7. T.W. Ebbesen and P.M. Ajayan: Large-scale synthesis of carbon nanotubes. *Nature* **358,** 220 (1992).
8. D. Ugarte: Morphology and structure of graphitic soot particles in arc-discharge C60 production. *Chem. Phys. Lett.* **198,** 596 (1992).
9. Y. Saito, T. Yoshikawa, M. Inagaki, M. Tomita, and T. Hayashi: Growth and structure of graphitic tubules and polyhedral particles in arc-discharge. *Chem. Phys. Lett.* **204,** 277 (1993).
10. R.S. Ruoff, D.C. Lorents, B. Chan, R. Malhorta, and S. Subramoney: Single crystal metals encapsulated in carbon nanoparticles. *Science* **259,** 346 (1993).
11. H. Shinohara, H. Sato, M. Ohkohchi, Y. Ando, T. Kodama, T. Shida, T. Kodama, T. Shida, T. Kato, and Y. Saito: Encapsulation of a scandium trimer in C82. *Nature* **357,** 52 (1992).
12. D.S. Bethune, R.D. Johnson, J.R. Salem, M.S. de Vries, and C.S. Yannoni: Atoms in carbon cages: The structure and properties of endohedral fullerenes. *Nature* **366,** 123 (1993).
13. Y. Saito, T. Yoshiokawa, M. Okuda, N. Fijimoto, S. Yamamuro, K. Wakoh, K. Sumiyama, K. Suzuki, A. Kasuy, and Y. Nishina: Iron particles nesting in carbon cages grown by arc-discharge. *Chem. Phys. Lett.* **212,** 379 (1993).
14. M. Tomita, Y. Saito, and T. Hayashi: LaC_2 encapsulated in graphite nano-particles. *Jpn. J. Appl. Phys.* **32,** L280 (1993).
15. S. Seraphin, D. Zhou, and J. Jiao: Filling the carbon nanocages. *J. Appl. Phys.* **80,** 2097 (1996).
16. A.K. Schaper, H. Hou, A. Greiner, R. Schneider, and F. Philipp: Copper nanoparticles encapsulated in multi-shell carbon cages. *Appl. Phys. A* **78,** 73 (2004).
17. J.S. Yu: Fabrication of bimodal porous silica with zeolite crystal core/mesoporous shell and corresponding nonspherical hollow carbon capsules. *Rev. Adv. Mat. Sci.* **10,** 341 (2005).
18. J.S. Yu, S.B. Yoon, Y.J. Lee, and K.B. Yoon: Fabrication of bimodal porous silicate with silicate-1 core/mesoporous shell structures and synthesis of nonspherical carbon and silica nanocases with hollow core/mesoporous shell structures. *J. Phys. Chem. B* **109,** 7040 (2005).
19. K. Ariga, A. Vinu, M. Miyahara, J.P. Hill, and T. Mori: One-pot separation of tea components through selective adsorption on pore-engineered nanocarbon, carbon nanocage. *J. Am. Chem. Soc.* **129,** 11022 (2007).
20. Q. Ji, M. Miyahara, J.P. Hill, S. Acharya, A. Vinu, S.B. Yoon, J.S. Yu, K. Sakamoto, and K. Ariga: Stimuli-free auto-modulated material release from mesoporous nanocompartment films. *J. Am. Chem. Soc.* **130,** 2376 (2008).
21. Z.M. Sheng and J.N. Wang: Thin-walled carbon nanocages: Direct growth, characterization and applications. *Adv. Mater.* **20,** 1071 (2008).
22. B.S. Xu and S.I. Tanaka: Formation of giant onion-like fullerene under Al nanoparticles by electron irradiation. *Acta Mater.* **46,** 5249 (1998).
23. E. Sutter, P. Sutter, and Y. Zhu: Assembly and interaction of Au/C core-shell nanostructures: In situ observation in the transmission electron microscope. *Nano Lett.* **5,** 2092 (2005).
24. R. Anton: In situ transmission-electron-microscopy study of the growth of Ni nanoparticles on amorphous carbon of the graphitization of the support in the presence of hydrogen. *J. Mater. Res.* **20,** 1837 (2005).
25. F. Banhart, J.C. Charlier, and P.M. Ajayan: Dynamical behavior of nickel atoms in graphitic networks. *Phys. Rev. Lett.* **84,** 686 (2000).
26. F. Banhart and P.M. Ajayan: Carbon onions as nanoscopic pressure cells for diamond formation. *Nature* **382,** 433 (1996).
27. Q. Jiang, N. Aya, and F.G. Shi: Nanotube size-dependent melting of single crystals in carbon nanotubes. *Appl. Phys. A* **64,** 627 (1997).

28. H. Baker: *Alloy Phase Diagram*, Vol. 3, ASM Handbook.
29. A.R. Badzian and A. Klokocki: On the catalytic growth of synthetic diamonds. *J. Cryst. Growth* **52,** 843 (1961).
30. G. Lulli, A. Parisini, and G. Mattei: Influence of electron-beam parameters on the radiation-induced formation of graphitic onions. *Ultramicroscopy* **60,** 187 (1995).
31. S. Hofmann, R. Sharma, C. Ducati, G. Du, C. Mattevi, C. Cepek, M. Cantoro, S. Pisana, A. Parvez, F. Cervantes-Sodi, A. Ferari, R. Dunin-Borkowski, S. Lizzit, L. Petaccia, A. Goldoni, and J. Robertson: In situ observations of catalyst dynamics during surface-bound carbon nanotube nucleation. *Nano Lett.* **7,** 602 (2007).